

Investigation of Speed Variation on Cavitation Phenomenon In Centrifugal Pumps Using Cosmos Flow Simulation

¹ Eng. Ahmed Saied Faheim, ² Prof. Dr. Abd El Fattah Mustafa Khourshid,
³Dr. Alaa-Eldin A.El-Hammady, ⁴Dr. Abdul Rahman Abdulla Badawi

¹. Assistant researcher, Mechanical & electrical research institute, National water research Centre, Egypt
². Mechanical Design Department, Faculty of Engineering, Tanta University
³. Mechanical Design Department, Faculty of Engineering, Tanta University
⁴. physical chemistry Department, National Research Center, Doke, Cairo, Egypt

Abstract

The objective of this paper is to present 3-D numerical study of the effect of speed variation on the cavitation phenomenon. The numerical computation in cavitating flow carried out using the (cosmos flow simulation within solidworks2013 CAD) is presented .The numerical simulation used the standard K- ϵ turbulence model to account for the turbulence effect. Pressure distribution and vapor volume fraction were obtained numerically at variable rotation speed .The numerical results showed that the cavitation phenomenon appeared at rotation speed 1500 rpm and increase effect with 3200 rpm.

Keywords: Cavitation phenomenon;centrifugal pumps; CFD; cosmos flow simulation; speed variation; solidworks.

Introduction

Cavitation is one of the disadvantages of the centrifugal pump. The cavitation phenomenon is an important cause of wear and damages in turbo machines. Cavitation occurs during the flow of water in the presence of regions of high flow velocity when local static pressure decreases below the vapor pressure.Motohiko[1], studied the cavitation flow in a low specific centrifugal pump speed by using two types of cavitation CFD codes.Okamura [2], used numerical cavitation content measurement and the validation of the bubble nucleation model.

prediction method available in commercial computational fluid dynamic software packages on the basis of a comparison of measurements obtained for a centrifugal pump.Nishi [3], used mini turbopump having its impeller diameter between 5 mm and 50 mm to find cavitation performance.

Calculation of incipient cavitation is simple as one has just to find the lowest pressure indicating the cavitation inception once this lowest pressure reaches the vapor pressure. According to Sudsuandee et al. [4], cavitation may occur on the blade suction surface in region of low pressure or at the runner leading edge at off-design operation. In a limited number of studies the effort was to simulate the cavitation in axial pumps. Mostafa, et al. [5], used an energy model to predict the cavitation erosion in centrifugal pumps, where they predicted the hydrodynamic aspect of cavitation. Fukaya, et al. [6] predicted the cavitation performance of an axial pump, but the model used does not include a turbulence model. Sedlář et al. [7], performed analysis of cavitation phenomena in water and estimated its application on prediction of cavitation erosion in hydraulic machinery. In the same article, the experimental research of the cavitating flow aiming to the validation of the erosion potential model is also shortly described, as well as development of the nuclei-

The main objective of this work is to study the effect of rotation speed variations on the cavitation phenomenon in centrifugal pump with specific interest in cavity geometry, pressure and

void fraction fields. Besides, the effects of turbulence and fluid viscosity are included. The cavity shape over the blades and the 3-D flow field around the cavitating propeller will be determined.

Theoretical Background (CAVITATION MODEL)

The basic approach is to use standard viscous flow (Navier-Stokes) equations with provisions for variable density and a conventional turbulence model, such as K- ϵ model. The latter is a numerical model developed by CFD-ACE+ solving (Navier-Stokes) equations [8].

Main Dimensions			
Number of blades	z		6
Hub diameter	DN	[mm]	21.5
Suction diameter	DS	[mm]	116
Impeller diameter	D2	[mm]	224
Outlet width	B2	[mm]	19.9
Work coefficient	ψ	[-]	0.95
Blade properties			
Thickness leading edge	sLE	[mm]	3.2
Thickness trailing edge	sTE	[mm]	3.7
Angle leading edge	β_1	[$^{\circ}$]	14.4
Angle trailing edge	β_2	[$^{\circ}$]	18.9

Table1: specification of centrifugal pumps.

The mixture density (ρ) is a function of vapor mass fraction (f), which is computed by solving a transport equation simultaneously with the mass and momentum conservation equations. The ρ - f relationship is:

$$\frac{1}{\rho} \equiv \frac{f}{\rho_v} + \frac{1}{\rho_l} \quad (1)$$

In two-phase flows, the use of vapor volume fraction (α) is also quite common. Therefore, it is deduced from f as follows:

This value is held constant throughout the calculation domain. However, the corresponding density (and hence volume fraction) varies significantly with local pressure. The perfect gas law is used to account for the expansion (or compressibility) of gas; i.e.

$$\alpha = f \frac{\rho}{\rho_v} \quad (2)$$

The transport equation for vapor is:

$$\frac{\partial}{\partial t}(\rho f) + \nabla \cdot (\rho f \vec{V}) = \nabla \cdot (\Gamma \nabla f) + R_e - R_c \quad (3)$$

The expressions of R_e and R_c have been derived from the reduced form of the Rayleigh-Plesset equation [8], which describes the dynamics of single bubble in an infinite liquid domain. The expressions for R_e and R_c are:

$$R_e = C_e \frac{V_b}{\sigma} - \rho_l \rho_v \sqrt{\frac{2p_{sat} - p}{3\rho_l}} (1 - f) \quad (4)$$

$$R_c = C_c \frac{V_b}{\sigma} - \rho_l \rho_v \sqrt{\frac{2p - p_{sat}}{3\rho_l}} f \quad (5)$$

Cavitation normally takes place in the vicinity of low pressure (or locally high velocity) regions, where turbulence effects are quite significant. In particular, turbulent pressure fluctuations have significant effect on cavitating flows. The magnitude of pressure fluctuations is estimated by using the following empirical correlation [9]:

$$\dot{p}_{turb} = 0.39 \rho k \quad (6)$$

The phasechange threshold pressure value is:

$$p_v = p_{sat} + 0.5 \dot{p}_{turb} \quad (7)$$

It is well known that cavitating flows are sensitive to the presence of non-condensable gases. In most liquids, there is a small amount of non-condensable gases present in dissolved and/or mixed state. For example, laboratory water generally has 15 ppm air dissolved in it. In other applications, e.g., marine propellers, etc., this amount may be considerably larger. In this model, the non-condensable gas is included by prescribing an estimated mass fraction at inlet.

$$\rho_{gas} = \frac{WP}{RT} \quad (8)$$

The calculation of mixture density (equation 1) is modified as:

$$\frac{1}{\rho} = \frac{f_v}{\rho_v} + \frac{f_g}{\rho_g} + \frac{1-f_g-f_v}{\rho_l} \quad (9)$$

Correspondingly, we have the following expression for the volume fractions of vapor (α_v) and gas (α_g):

$$\alpha_v = f_v \frac{\rho}{\rho_v} \quad (10)$$

$$\alpha_g = f_g \frac{\rho}{\rho_g} \quad (11)$$

And,

$$\alpha_l = 1 - \alpha_v - \alpha_g \quad (12)$$

The combined volume fraction of vapor and gas (i.e., $\alpha_v + \alpha_g$) is referred as the Void Fraction (α). In practical applications, for qualitative assessment of the extent and location of cavitation, contour maps of void fraction (α) are important for bubbles location and shape determination.

Computational Analysis

Numerical simulation was performed using a 3-D cosmos flow simulation within solidworks2013 CAD.

The turbulence modeling in COSMOS is done using the K- ϵ model. The K- ϵ model is one of the most commonly used as it offers a reasonable compromise between computational effort and accuracy [9]. It is based on the solution of equations for the turbulent kinetic energy K and the turbulent dissipation rate ϵ [10].

It is clear that the full cavitation model used in this simulation includes a plethora of effects ignored in previous studies, such as unsteady, fluid viscosity, turbulence and variation of rotation speed factor.

Computation Domain And Boundary Condition

The boundary condition as shown in Figure 1 is important to represent the flow in the centrifugal pump for CFD analysis to begin. CFD results are usually related to the number of cells used to model the flow.

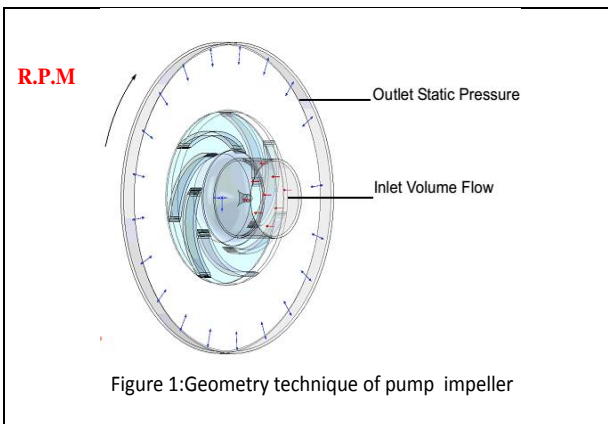
Proper boundary condition is determined for the simulation and after the design of the centrifugal pump is finished, the design is transferred to COSMOS Flow Works for analysis [11]. Before the analysis was done, a set of the boundary condition of the dissolve of gases (Air) in water is established. The CFD software utilizes the Navier Stokes equations to solve the flow behavior [12]. The boundary condition consists of two walls, inlet and outlet at blade and hub surface, smooth relative frame stationary wall is selected as a default boundary condition. At shroud surface, relative frame counter rotating wall is applied with Log-Law wall model and smooth wall. Inlet boundary condition absolute total pressure is set include of specification of turbulent intensity and length scale. Direction of absolute flow is defined in Cartesian coordinate. At the outlet, a mass flow for one passage is specified.

These are some boundary condition that has been setup during the analysis:

The rotation speed: (750, 1500&3200r.p.m).

Cavitation on with Dissolved gas mass fraction: 0.001

After keying in these input parameters, calculation were done with 801 iteration before the result were out.



The rotation speed were 750, 1500 and 3200rpm. In order to simulate the rotation in the structured grid of the rotor, a rotating frame of the grid was assumed around the rotor axis. The

computer used was Intel Core i5 Processor 2.4 GHz, and 3 GB RAM.

Results and Discussion

The contours of computed vapor volume fraction on the blades at variation speed 750, 1500, and 3200 rpm are presented in figure 2 a, b, c respectively. The static pressure decreases sharply below the vapor pressure at the leading edge of the blades at speed 1500 rpm and increasing at 3200 rpm, while the static pressure at speed 750 rpm is above the vapor pressure.

The average volume fraction of vapor distribution on chord length of the blade at variable rotation speed is shown in figure 4. The vapor volume fraction increases at the leading edge of the blades at rotation speed and its increasing sharply 3200 rpm, while at rotation speed 750 rpm is equal to zero. The total pressure decreasing below the vapor pressure at the leading edge of the blades at rotation speed 1500 rpm and its decreases sharply 3200 rpm while at rotation speed 750 rpm is above the vapor pressure.

It is obvious that cavitation does not appear at rotation speed 750 rpm while it is present at rotation speed 1500 and 3200 rpm at the leading edge of the suction side due to the decrease in static pressure below the vapor pressure. The computed density contours on the rotor at rotation speed 750, 1500, 3200 rpm are presented in figure 3 a, b, c respectively. It is obvious that is not change in a density at rotation speed 750 rpm, while the density decreases at rotation speed 1500 r.p.m and decreases sharply at rotation speed 3200 rpm at the leading edge of the blades due to the decrease in static pressure below the vapor pressure. The Average density distribution on chord length of the blade at variable rotation speed is shown in figure 4. Again, there is no density change at rotation speed 750 rpm, while the density decreases at the leading edge suction of the blades at rotation speed 1500 rpm and decreases sharply at 3200 rpm.

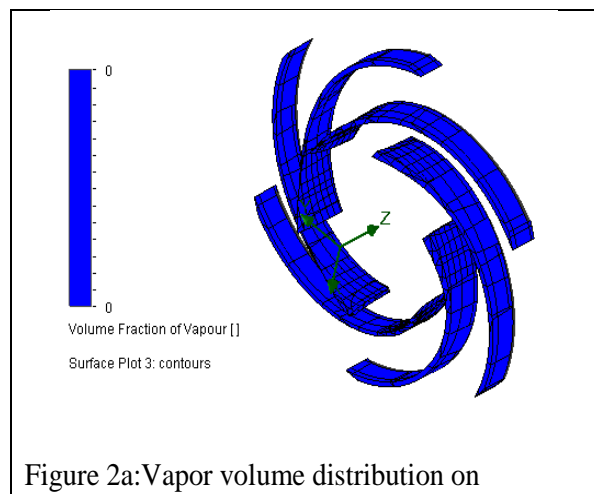


Figure 2a: Vapor volume distribution on the blades at 500 rpm

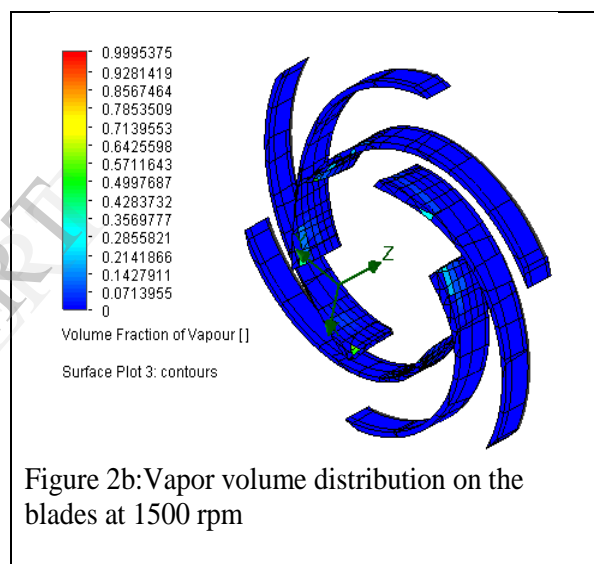


Figure 2b: Vapor volume distribution on the blades at 1500 rpm

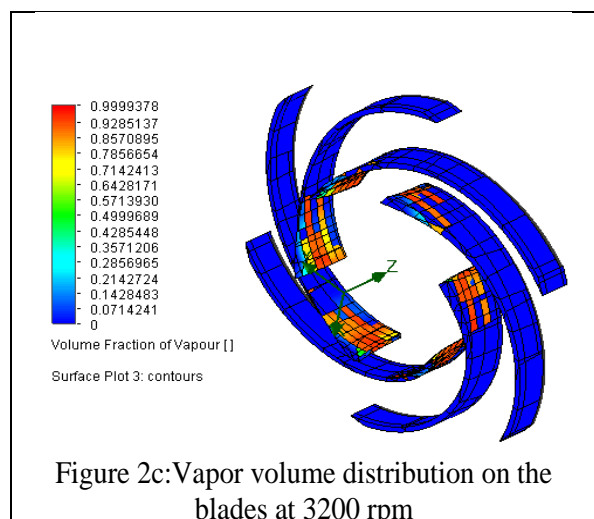
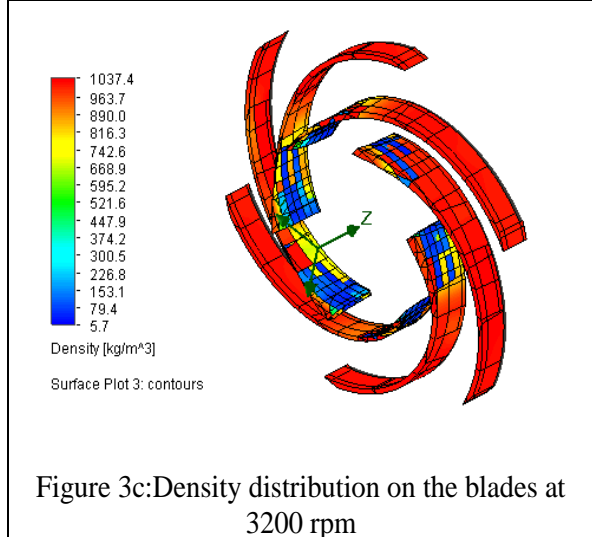
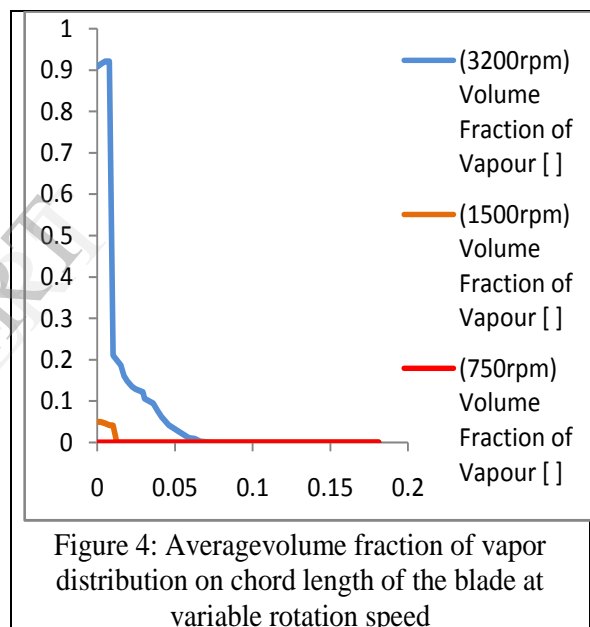
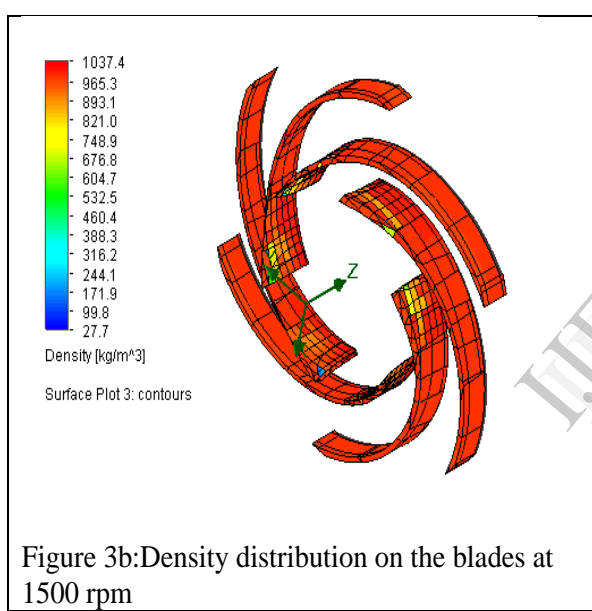
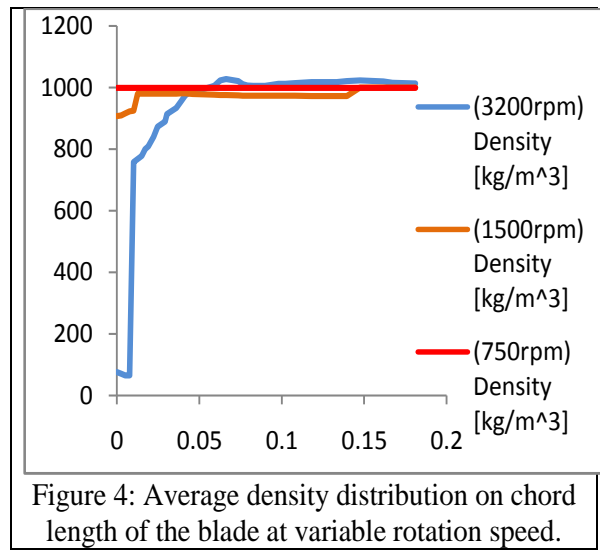
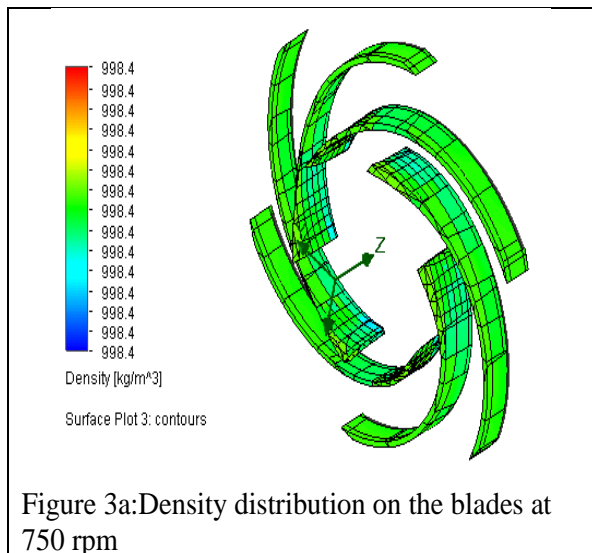


Figure 2c: Vapor volume distribution on the blades at 3200 rpm



Summary and Conclusions

The CFD results computed by cosmos flow simulation within solidworks2013 CAD software can be shown that the formation bubble form in a lower pressure area which caused by high velocity fluid. Inception cavitation occurs on the blade surface where the leading edge meets the tip at high rotational speed with presence of air mixed with water.

The results show that tip cavitation can directly lead to losses in efficiency, especially for flow rates inside the cavitation zone

Nomenclature

C_c	Phase change rate coefficients	
C_N	Slip speed factor "ratio between impeller actual rotational speed and theoretical rotating frame speed"	
f	Vapor mass fraction	
K	Turbulence kinetic energy	m^2/s^2
N	Pump rotational speed	rpm
P	Fluid static pressure	N/m^2
p_{sat}	Saturation pressure	N/m^2
P'_{turb}	The magnitude of pressure fluctuations	N/m^2
P_t	Total pressure	N/m^2
P_v	Vapor pressure	N/m^2
R	Universal gas constant	$Nm/Kg.k$
R	Phase change rate	
Re	Reynolds number	
T	Fluid temperature	K
Δt	Physical time step	s
W	Molecular weight	$Kg/Kg\text{-mol}$

Greek Letters

β_1	Blade inlet angle (angle between the tangent to camber line at inlet and the axial direction)	degree
β_2	Blade outlet angle (angle between the tangent to camber line at outlet and the axial direction)	degree
α_v	Vapor volume fraction	
α_g	gas volume fraction	
σ	Cavitation number $((p_w - p_v) / (1/2 \rho \mu^2))$	--
ρ	The mixture density	Kg/m^3

Suffixes

c	Bubble reduction and collapse
e	Bubble generation and expansion
Gas, G	Gaseous phase
L	Liquid phase
V	Vapor phases

References

[1] Motohiko Nohmi 2003" Cavitation CFD in A Centrifugal Pump" Fifth International Symposium on Cavitation Osaka, Japan.

[2] Tomoyoshi Okamura 2003" Cavitating Flow Calculations in Industry" International Journal of Rotating Machinery, 9(3): pp 163 – 170.

[3] Michihiro Nishi 2003" Cavitation Performance of a Centrifugal Impeller Suitable for a Mini Turbo-Pump" Fifth International Symposium on Cavitation Osaka, Japan.

[4] Sy Sudsuwansee T, Nontakaew U, Tiaple Y (2011) Simulation of leading edge cavitation on bulb turbine. Songklanakarin J SciTechnol 33: 51-60.

[5] Mostafa NH, Rayan MA, Mahgob MM (1990) Energetic model for cavitation erosion prediction in centrifugal pump impeller. Proceeding of ASME/CSME Cavitation and Multiphase flow forum, Toronto, Canada.

[6] Fukaya M, Okamura T, Tamura Y, Matsumoto Y (2003) Prediction of Cavitation Performance of Axial Flow Pump by Using Numerical Cavitating Flow Simulation with Bubble Flow Model. Fifth International Symposium on Cavitation, Osaka, Japan.

[7] Sedlář M, Zima P, Němec T, Maršík F (2008) Analysis of Cavitation Phenomena in Water and its Application to Prediction of Cavitation Erosion in Hydraulic Machinery. ICPWS XV, Berlin.

[8] Hinze JO (1975) Turbulence. (2nd Edn) McGraw-Hill Book Company, New York, USA.

[9] Blazek, J., Computational Fluid Dynamics: Principles and Applications, Second Edition, page 55

[10] Blazek, J., Computational Fluid Dynamics: Principles and Applications, Second Edition, page 243

[11] CosmosTM, "Technical Reference Manual", COSMOSFloWorsFundamentals., 2012.

[12] Bo Yan Xu, Mikio Furuyama, "Visualization of Natural Gas-Air Mixing Flow in the Mixer of a CNG Vehicle", Technical Notes, JSAE Review 18 57-82, 1997